CORE
Metadata, citation and similar papers at core.ac.uk
Provided by Elsevier - Publisher Connector

FEBS Letters 581 (2007) 4495–4500

Functional analyses of the extra- and intracellular domains of the yeast cell wall integrity sensors Mid2 and Wsc1

Andrea Straede, Jürgen J. Heinisch*

Universität Osnabrück, Fachbereich Biologie/Chemie, AG Genetik, Barbarastr. 11, D-49076 Osnabrück, Germany

Received 8 May 2007; revised 12 July 2007; accepted 13 August 2007

Available online 22 August 2007

Edited by Judit Ovádi

Abstract **Cell wall integrity signalling in *Saccharomyces cerevisiae* provides a model for the regulation of fungal wall biosynthesis. Chimers of the major plasma membrane sensors Wsc1 and Mid2 fused to GFP have been employed to show that intracellular and membrane distribution is only dependent on a membrane-anchored cytoplasmic tail. Phenotypic analyses of chimeric sensors in an isogenic Δ*mid2* Δ*wsc1* double deletion strain indicate that this tail, provided that it is linked to an extracellular domain, also determines the cellular response to different surface stresses to a large extent.**
© 2007 Federation of European Biochemical Societies. Published by Elsevier B.V. All rights reserved.

Keywords: Yeast; Stress; Wsc1/Slg1; Mid2

1. Introduction

Cell integrity in fungi is mainly ensured by a rigid cell wall, which represents a potential target for antifungal drugs [1,2]. In yeasts, such as *Saccharomyces cerevisiae*, the cell wall is subject to controlled structural changes during growth and mating [3]. This cell wall remodelling can also be observed during cell surface stress. Detection of the latter is achieved by a set of plasma membrane sensors which, through the sole yeast protein kinase C (Pkc1), are connected to a conserved mitogen activated protein kinase (MAPK) cascade (reviewed in [4,5]). Activation of the MAPK module finally results in transcriptional changes which lead to new cell wall biosynthesis. Mutations in many genes which encode components of this so-called cell wall integrity (CWI) pathway cause a cell lysis defect which is osmo-remedial. They are also hyper-sensitive to cell wall destabilizing compounds such as Calcofluor white (CFW) and Congo red [6], as well as to agents which act on the plasma membrane, such as sodium dodecyl sulfate (SDS) and tea tree oil [7].

The exact molecular mechanisms by which such stresses are detected by the plasma membrane sensors still remains elusive. Two small families of sensors have been described which are able to activate the afore mentioned intracellular signalling cascade: Three members of the Wsc-family (Wsc1, Wsc2 and Wsc3; for "wall stress component") have been identified in different genetic screens [8–10] (note that Wsc1 is synonymous with Slg1 and Hcs77). They are characterized by a cysteine-motif near the amino terminal end, which is followed by a serine/threonine-rich, highly mannosylated extracellular region, a single transmembrane domain (TMD) and a relatively short cytoplasmic tail [11–13]. Each of these motifs has been shown to be essential for in vivo-function in deletion analyses [14]. The second group of sensors is constituted by Mid2 and Mtl1 [11,13]. Despite low primary sequence similarities, the overall structure of these sensors is reminiscent of the Wsc-family, but they lack the cysteine-motif (see [5], and references therein). It is presumed that the cysteines could establish a contact to the cell wall glucans and that the glycosylation of the Ser/Thr-region confers a rod-like structure (reviewed in [5]). The cytoplasmic tails of Wsc1 and Mid2 have been shown in yeast two-hybrid assays to interact with Rom2, the GDP/GTP exchange factor (GEF) which mediates activation of the small GTPase Rho1 and hence that of the subsequent CWI components [15,16].

Genetic analyses indicate a primary importance of Wsc1 and Mid2 for CWI signalling [10,13]. Defects in the other redundant sensors do not display significantly increased stress sensitivities as compared to the wild-type, but mainly aggravate those of null mutants in either *WSC1* or *MID2*. Since overexpression of *MID2* partially complements the deletion of *WSC1*, it has been concluded that the sensors serve different, but overlapping functions [11,13]. In this work, we aimed to follow up these investigations by determining the specificity of chimeric Wsc1/Mid2 sensors for different stress agents. In addition, we investigated the influence of the cytoplasmic tail on the intracellular distribution of functional sensor-GFP fusions.

2. Materials and methods

2.1. Media, growth conditions, strains and genetic manipulations

Unless stated otherwise, media and standard procedures were applied as recently described [7]. Caspofungin (brand name Cancidas; Merck & Co. Inc., USA; 50 mg) was obtained from a local pharmacy and prepared in sterile water according to the instructions of the manufacturer. It was added to rich medium (YEPD) after autoclaving and cooling, to final concentrations of 50 and 100 ng/ml. *S. cerevisiae* strains employed in this work are HAS17-3B (*MATα ura3-52 leu2-3,112 his3-11,15*; an isogenic derivative of HD56-5A [17]) and the isogenic deletion mutants HAS17-3C (*MATα ura3-52 leu2-3,112 his3-11,15 wsc1*::*SpHIS5*), HAS17-3A (*MATα ura3-52 leu2-3, 112 his3-11,15 mid2*::*KlLEU2*), and HAS17-3D (*MAT**a** ura3-52*

*Corresponding author. Fax: +49 541 969 2349.
E-mail address: heinisch@biologie.uni-osnabrueck.de (J.J. Heinisch).

Abbreviations: CFW, calcofluor white; CWI, cell wall integrity; GEF, GDP/GTP exchange factor; MAPK, mitogen activated protein kinase; nt, nucleotide; SDS, sodium dodecyl sulfate; TMD, transmembrane domain; TTO, tea tree oil; $Wsc1_{ex}$–$Mid2_{cyt}$, external sequences and TMD with cytoplasmic tail of the respective sensors

0014-5793/$32.00 © 2007 Federation of European Biochemical Societies. Published by Elsevier B.V. All rights reserved.
doi:10.1016/j.febslet.2007.08.027

leu2-3,112 his3-11,15 wsc1::*SpHIS5 mid2*::*KlLEU2*) [7]. HAS17-3D was used as a recipient strain to construct different sensor gene variants. Consequently, the following strains share all the auxotrophic markers and only the sensor alleles are indicated: HAS28 (*mid2*::*MID2*$_{ex}$–*WSC1*$_{cyt}$-*kanMX wsc1*::*SpHIS5*), HAS29 (*mid2*::*KlLEU2 wsc1*::*WSC1*$_{ex}$–*MID2*$_{cyt}$-*kanMX*), HAS43 (*mid2*::*MID2*$_{cyt}$-*kanMX wsc1*::*SpHIS5*) and HAS44 (*mid2*::*KlLEU2 wsc1*::*WSC1*$_{cyt}$-*kanMX*) were obtained by one-step gene replacement using appropriate fragments of the plasmids pAS39, pAS40, pAS51 and pAS52 (see below), respectively. For work with *Escherichia coli*, strain DH5α from Invitrogen (Karlsruhe/Germany) was used.

2.2. Plasmids, genomic substitutions, GFP fusions and sequence analyses

In order to obtain the genes which encode chimeric sensors on plasmids suitable for genomic replacement of the deletion alleles, derivatives of pUG6 [18] were constructed, with sensor sequences flanking the *kanMX* marker cassette.

For this purpose, fragments which contain the 5′ ends of the sensor genes (with approximately 100 bp upstream of the coding sequence and the entire open reading frame) were inserted upstream. Downstream of the cassette, approximately 500 bp of non-coding sequences 3′ of the sensor genes were introduced: The plasmid pAS31 (*MID2*) was constructed with PCR products made with the oligonucleotide pairs 04.98/04.99 (upstream) and 04.100/04.101 (downstream), which were cloned into the vector pUG6 using the restriction sites underlined in the oligonucleotides listed in Table 1. With the oligonucleotides 04.128 and 04.129 a BamHI-recognition sequence was introduced into the *MID2*-sequence with the "QuikChange site-directed mutagenesis kit" (Stratagene, La Jolla, USA). Similarly, pAS30 (*WSC1*) was constructed from pUG6 with PCR products obtained with the oligonucleotides 04.94/04.95 (upstream sequences with entire open reading frame including 200 bp of the 5′ non-coding region; restriction sites underlined in Table 1), and 04.96/04.97 (approximately 800 bp within the downstream non-coding region; for cloning into pUG6 XhoI and EcoRV, which are intrinsic to the amplified sequences, were used in this case). The BamHI site was introduced by site directed mutagenesis with the oligonucleotides 04.126/04.127. To this end, pAS30 and pAS31 were digested with BamHI/XbaI and the obtained fragments were exchanged to get pAS39 (*MID2*$_{ex}$–*WSC1*$_{cyt}$) and pAS40 (*WSC1*$_{ex}$–*MID2*$_{cyt}$). Furthermore, the sequences encoding the external sensor domains were deleted. Therefore, pAS30 and pAS31 were used as templates for an inverse PCR reaction using the oligonucleotides 05.210/04.128 and 05.209/04.126, which introduced additional BamHI sites after the sequence encoding the signal peptide of each sensor. The PCR products were digested with BamHI and religated to yield plasmids pAS51 (*MID2*$_{cyt}$) and pAS52 (*WSC1*$_{cyt}$). DNA sequences were provided by Heinz Gabriel (Osnabrück/Germany) for which custom-made oligonucleotides from MWG-Biotech (Munich/Germany) were employed.

Genomic C-terminal GFP-fusions of wild-type *WSC1* and *MID2* in strain HD56-5A were obtained *via* homologous recombination with PCR products obtained from pFA6a-GFP (S65T)-kanMX [19] as template and the oligonucleotide pairs 03.50/03.51 (*WSC1-GFP*) and 03.52/03.53 (*MID2-GFP*) as listed in Table 1. Segregants from crosses with isogenic strains yielded HAS35-8D (*MAT***a** *WSC1-GFP*::*kanMX ura3-52 leu2-3,112 his3-11,15*) and HAS4011A (*MATα MID2-GFP*::*kanMX ura3-52 leu2-3,112 his3-11,15*). Strains which produce carboxy-terminal sensor GFP fusions of the chimeric sensors were obtained from the strains described above as follows: HAS50 was derived from HAS28 by transformation with a BamHI/SalI fragment from pAS59. The latter contains the 3′ part of the *WSC1* coding sequence (from nt 742 to 1134 counted from the ATG translation start codon) fused in frame to GFP derived from pKT209 [20], followed by a *Candida albicans URA3* cassette and a *MID2* 3′ non-coding region (from nt 255 to 326 after the translation stop codon). pAS59 was obtained through several subcloning steps (details are available upon request).

HAS49 was derived from HAS29 by transformation with a BamHI/SalI fragment from pAS57. The latter contains the 3′ part of the *MID2* coding sequence (from nt 613 to 1128 counted from the ATG translation start codon) fused in frame to GFP derived from pKT209, followed by a *CaURA3* cassette and a *WSC1* 3′ non-coding region (from nt 700 to 905 after the translation stop codon). pAS57 was obtained through several subcloning steps (details are available upon request).

HAS51 was obtained from HAS43. To this end, the BamHI/HindIII fragment from pAS81 was transformed. The latter contains the same *WSC1* and GFP coding sequences as pAS59, followed by a *Kluyveromyces lactis URA3* cassette and the *WSC1* non-coding region from pAS30.

HAS52 was derived from HAS44 by transformation with the BamHI/HindIII fragment from pAS83. The latter contains the same *MID2* and GFP coding sequences as pAS57, followed by a *KlURA3* cassette and the *MID2* non-coding region from pAS31.

2.3. Fluorescence microscopy

For fluorescence microscopy, cells were grown overnight in synthetic medium and then inoculated for another 3–6 h in fresh medium with shaking at 25 °C. Equipment and imaging conditions have been described, previously [21].

3. Results

3.1. Functional characterization of chimeric sensors

Mutants defective in different components of the CWI pathway display considerable phenotypic variations depending on

Table 1
Oligonucleotides used in this work

Name	Sequence (5′–3′)
03.50	accaggagggaaaaacaacgtttaacagtggtcaatccagacgaagctgatCGGATCCCCGGGTTAATTAA
03.51	ggagatgatttggcaaaatgaaatcggaaaaagaaaaaattaatgggaagGAATTCGAGCTCGTTTAAAC
03.52	gaagaaaaattctatgatgaacaaggtaacgaattatcaccacgaaattatCGGATCCCCGGGTTAATTAA
03.53	gtccacctactcaatatcagaaatataattaagatggtcaatttacaataattGAATTCGAGCTCGTTTAAAC
04.94	gcgcgtcGACCAGGCACTAACATTACAG
04.95	gcgctctagaCCTCGTTACTTCCAGCTCTCCAGC
04.96	GCGCAAGGATTGATTATGTGATAGG
04.97	GTAGTTTACAATAAGGGCAGC
04.98	cgcggtcGACGCCTCTGCCTCAAAGACATAC
04.99	cgcgtctaGAGGGTATGTAATGCTAATCCTAC
04.100	cgcgcTCGAGTGCTTTAACGTTCCACTG
04.101	cgcgactAGTTATTCCCTTTTGCGTCGTC
04.126	GGTACAGCTGGATCcGACTCTACGAGTGG
04.127	CCACTCGTAGAGTCgGATCCAGCTGTACC
04.128	CTACCGTTACGTACACAggATCcGCAACCGCTGATTCAAGC
04.129	GCTTGAATCAGCGGTTGCgGATccTGTGTACGTAACGGTAG
05.209	gcccggatccTTGCACGAAAAATTGTGCGCG
05.210	gcccggatccTAGTGAGCTAAAACAATTCACG

Restriction recognition sequences introduced by the oligonucleotides and used for subcloning are underlined. Small print indicates nucleotides not present in the template sequence.

their genetic background (see [22], and references therein). Therefore, the studies reported in this work are exclusively based on an isogenic series of strains, which differed only with respect to the sequences at the *WSC1, MID2* and *MAT* loci [7]. The Δ*mid2* Δ*wsc1* double deletion strain HAS17-3D was used as a recipient to genomically replace the null alleles by various parts of one or the other sensor by in vivo recombination (Fig. 1A). First, the functional importance of the large extracellular domain of each sensor in the genetic background of this strains was determined. Therefore, sequences which encode the signal peptide in frame with the TMD and the cytoplasmic tail of Wsc1 and Mid2, tagged with a *KanMX* marker, were used to substitute the *wsc1*::*SpHIS5* and the *mid2*::*KlLEU2* deletions, respectively. By the use of GFP-fusions, the proteins produced were shown to reside at the plasma membrane (see below). As shown in Fig. 1B the Δ*mid2* Δ*wsc1* double deletion strain was sensitive to all stress conditions and only grew in the presence of osmotic stabilization, i.e. on plates containing 1 M sorbitol. Similar phenotypes can be observed for strains carrying the truncated constructs. In contrast, the wild-type and the Δ*mid2* strain grew well in the presence of caffeine, Calcofluor white, SDS, and at elevated temperatures. For tea tree oil, the reported hyper-resistance of the Δ*mid2* deletion mutant was observed [7]. For caspofungin, both single deletion strains showed sensitivity as compared to the wild-type. On the other hand, the strain with a Δ*wsc1* deletion displayed an increased sensitivity to caffeine and Calcofluor white. Thus, each sensor deletion mutant responds to a

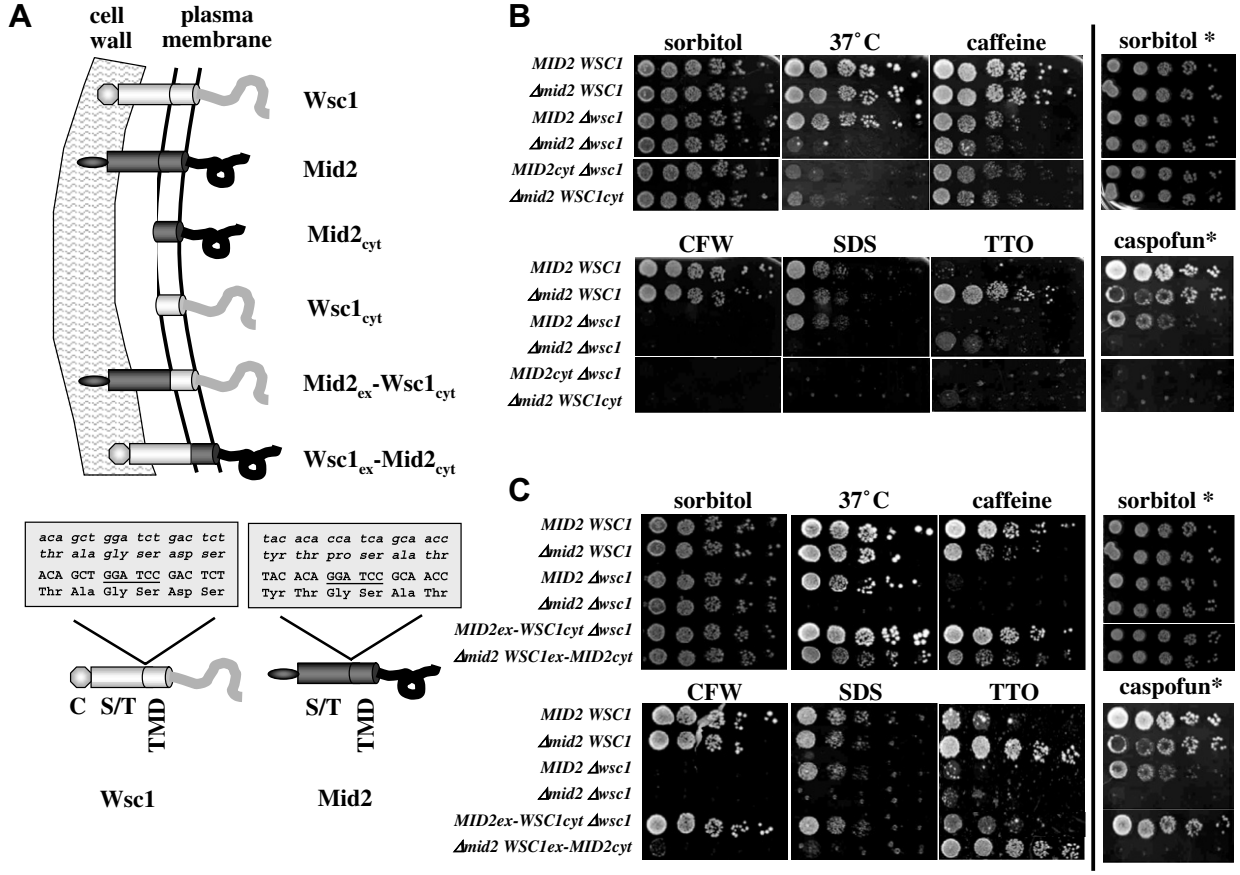

Fig. 1. Phenotypic analyses of strains with different sensor genes. (A) Schematic representation of sensor variants expressed in the background of the Δ*mid2* Δ*wsc1* double deletion strain HAS17-3D. The Wsc1 sensor is depicted in light grey, the Mid2 sensor in dark grey. Below, the modified DNA and protein sequences obtained by the introduction of the BamHI sites (underlined) for construction of the chimeric sensors are indicated. Small print and italics represent the original DNA and protein sequences in this region. Capital letters of DNA and amino acids represent the sequence after introduction of the restriction site. C designates the cysteine motif, S/T the serine/threonine-rich region, and TMD the transmembrane domain. The different sensor domains are not drawn according to scale. (B, C) Serial dilution patch tests of the strains are shown. All plates contained rich medium (YEPD) and were incubated at 25 °C, if not indicated otherwise. Plates were incubated for 3–4 days. Caffeine was added at a final concentration of 7.5 mM, SDS at 0.1%, and tea tree oil (TTO) at 0.2%, the latter in conjunction with 0.5% Tween 40. Due to the enormous charge variations in commercially available preparations of Calcofluor white, the plate shown in (B) contained 300 μg/ml, the one shown in (C) only 10 μg/ml. (B) Phenotypes of strains with externally truncated Wsc1 and Mid2 sensors. Drop dilution assays are all from the same experiment and from one plate for each condition. Strains tested were (from top to bottom): HAS17-3B, HAS17-3A, HAS17-3C, HAS17-3D, HAS43, HAS44. (C) Investigation of chimeric sensor constructs. Note that the plate containing TTO was obtained from an independent assay and was incubated for 6 days in this case. Strains tested were (from top to bottom): HAS17-3B, HAS17-3A, HAS17-3C, HAS17-3D, HAS28, HAS29. *Designates results from an independent experiment to determine the effect of caspofungin. The plates shown are either the controls in the presence of osmotic stabilization (YEPD/sorbitol) or rich medium (YEPD) containing 50 ng/ml caspofungin (caspofun). All plates were incubated for 3 days at 25 °C. Note that the upper 4 lanes in (B) and (C) show the control strains and are from one assay (i.e. identical). The lower two lanes were assayed in the same experiment on the same plates and show the strains with modified sensor genes. At 100 ng/ml caspofungin only the wild-type strain was able to grow, and HAS43 (*MID2*$_{ex}$–*WSC1*$_{cyt}$ Δ*wsc1*) displayed a marginal resistance (not shown).

specific set of stress conditions and the membrane-anchored cytoplasmic tails are not sufficient to complement the growth defects of the double deletion.

To investigate which parts of the sensors determine signal specificity, the extracellular sequences of Wsc1 were fused to the TMD and cytoplasmic tail of Mid2 and *vice versa*. Again, all encoding constructs were genomically integrated at the respective loci (i.e. $WSC1_{ex}$–$MID2_{cyt}$ at the *WSC1* locus and $MID2_{ex}$–$WSC1_{cyt}$ at the *MID2* locus). As evident from Fig. 1C, a strain with a chimeric sensor carrying the cytoplasmic tail of Wsc1 grows like the wild-type control under almost all conditions tested. In this respect, the chimeric construct behaves much like a strain carrying a single Δ*mid2* deletion. However, it does not display a hyper-resistance to tea tree oil. On the other hand, a strain expressing a fusion of the extracellular domain of Wsc1 to the internal part of Mid2 ($WSC1_{ex}$–$MID2_{cyt}$) largely resembles the single Δ*wsc1* deletion strain in its growth behaviour (i.e. in the presence of Calcofluor white, caspofungin and at elevated growth temperatures). It is, however, slightly more sensitive to SDS, slightly more resistant to caffeine and displays a remarkable hyper-resistance to tea tree oil (Fig. 1B). Note that for the single deletion mutants variations with respect to caffeine-sensitivity can be observed between independent experiments. Therefore, all tests always included the proper controls.

3.2. Intracellular sensor distribution

In order to obtain some information on the governing factors regarding the dynamics and intracellular localization of the sensors, the wild-type genes and those which encode the truncated and the chimeric sensors described above were genomically fused in frame to the *GFP* gene at their 3′ end. The carboxyterminal GFP-modification of the full-length sensors did not alter the growth behaviour of the strains with the non-tagged versions under any of the conditions tested above (data not shown). This can be taken as strong evidence that the fusions are functional *in vivo*. Wsc1-GFP proved to be highly dynamic and concentrated at emerging buds and at the bud neck prior to cytokinesis (Fig. 2). On the other hand, Mid2-GFP showed a more static, even membrane distribution.

Interestingly, the GFP-fusions of the membrane-anchored constructs completely lacking the extracellular domain local-

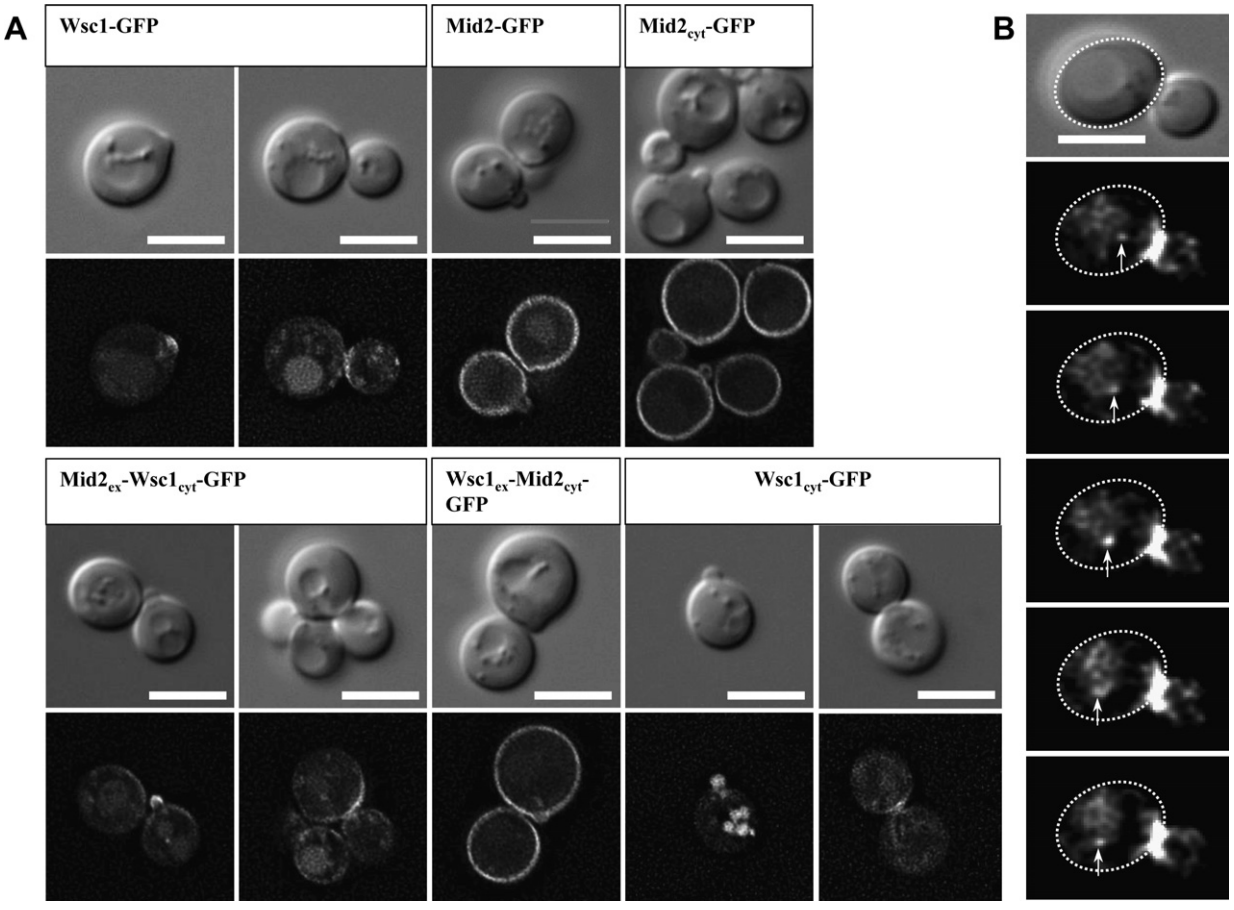

Fig. 2. Localization of different sensor-GFP fusions. (A) The upper lanes show the bright field images, the lower lanes the GFP fluorescence. The white bars represent a size standard of 5 μm. For Wsc1-GFP constructs two pictures are shown on the left as examples of localization at the emerging bud and at the bud neck and vacuole prior to cytokinesis, respectively. Note that in the fusion with only the cytoplasmic tail of Wsc1 both a localization at the emerging bud and in fragmented vacuolar compartments can be observed. Strains employed were: HAS35-8D (Wsc1–GFP), HAS40-11A (Mid2-GFP), HAS51 ($Mid2_{cyt}$–GFP), HAS50 ($Mid2_{ex}$–$Wsc1_{cyt}$–GFP), HAS49 ($Wsc1_{ex}$–$Mid2_{cyt}$–GFP), HAS52 ($Wsc1_{cyt}$–GFP). (B) Time-lapse pictures of HAS35-8D (Wsc1-GFP). The uppermost picture shows the bright-field image (size bar = 4 μm) and the following images from top to bottom were taken from the same cell with the GFP-filter in time intervals of 800 milliseconds. The white doted line which surrounds the mother cell has been superimposed for orientation. The arrow indicates one signal changing its position. Note that other signals are also changing in the same time frame.

ized much like the full-length fusions. Thus, $Wsc1_{cyt}$-GFP concentrated at the sites of emerging buds and, subsequently, at the bud neck. There appeared to be a highly dynamic fluctuation between plasma membrane and cytoplasm. In addition, a marked accumulation of the GFP signal can be detected within the vacuole, which, besides endocytic travelling, could also be due to a misfolding of the protein in the secretory pathway and targeting for degradation (Fig. 2). $Mid2_{cyt}$-GFP showed the static membrane distribution as did the full-length Mid2-GFP fusion. Finally, GFP-fusions of the chimeric sensors also behaved as expected from the information displayed by their cytoplasmic tails. Thus, $Mid2_{ex}$–$Wsc1_{cyt}$-GFP showed the dynamic distribution observed for Wsc1-GFP and external sequences and TMD with cytoplasmic tail of the respective sensors ($Wsc1_{ex}$–$Mid2_{cyt}$)-GFP appeared across the entire plasma membrane, as did Mid2-GFP.

To determine the contribution of the TMD to sensor localization, we also constructed genomic GFP fusions switching only the intracellular domains of the sensors. Again, hybrid sensors with only the cytoplasmic tail of Wsc1 ($Mid2_{exTMD}$–$Wsc1_{cyt}$) resembled $Wsc1_{cyt}$-GFP (which lacks the external domain) in its distribution and dynamics, and those with only the cytoplasmic tail of Mid2 behaved like Mid2-GFP (data not shown).

4. Discussion

The exact mode by which the CWI sensors Mid2 and Wsc1 recognize extracellular signals and trigger specific intracellular responses in *S. cerevisiae* is still a mystery [5]. An appealing model for these functions is deduced from the similar sensor structures. Thus, the amino-terminal ends of the sensors could bind to cell wall components (through the cysteine-motif of Wsc1 and an as yet unknown mode of action for Mid2). The highly mannosylated Ser/Thr-rich region could provide a rod-like structure connecting to the TMD. Mechanical forces acting either on the cell wall or on the plasma membrane would then trigger a protein distortion, which in turn may alter the folding of the cytoplasmic tail. Alternatively, the signal could lead to a dimerization of the sensor molecules also affecting the conformation (or modification [23]) of the cytoplasmic regions. The latter would, either directly or indirectly, allow interaction with Rom2 as an upstream component of the CWI signalling pathway [16,23]. Although such a model provides a means of signal detection, it does not explain the sensor-specific cellular responses.

The phenotypes of the chimers investigated in this work indicate that the cytoplasmic tails of the sensors contribute significantly to the signal specificity. Note that a Δ*mid2* deletion in the genetic background of our strain does not show reduced growth under most of the conditions tested. A reported hyper-resistance to caspofungin [24] was not observed. Rather, the deletion strain was more sensitive as compared to the wild-type. Therefore the conclusion on the importance of the cytoplasmic tail for signalling is mainly taken from the phenotypes conferred by the construct carrying this tail derived from Wsc1 ($Mid2_{ex}$–$Wsc1_{cyt}$). It rescued most of the growth defects displayed by the double deletion strain (*wsc1*::*SpHIS5 mid2*::⇌*KlLEU2*). The failure to complement, which was observed with the sensors lacking the external sequences, clearly shows that an external extension (which is interchangeable between the sensors and most likely connects to the cell wall) is essential for function. This adds to the previous observations reported on truncated Wsc1 sensors [14,16,25]. However, it should be noted that, with regard to tea tree oil, the extracellular part of the sensor seems to govern the response, i.e. the $WSC1_{ex}$–$MID2_{cyt}$ construct shows the hyper-resistance of a Δ*mid2* deletion strain. Thus, specificity also seems to depend on the type of extracellular stress applied.

In this context, an appealing way to modulate the cellular response to stresses detected by different sensors through the same CWI signalling pathway would be a micro-compartmentation within the plasma membrane. Thus, local sensor concentrations could lower the threshhold for signal generation. In fact, as demonstrated with the C-terminal GFP fusions, Wsc1 and Mid2 display a strikingly different dynamics and localization within the plasma membrane. The highly dynamic behaviour of Wsc1 has recently been shown to be caused by a fast turnover through endocytosis ([26] and unpublished results from our laboratory). This was also observed for the homologous sensor from the closely related yeast *Kluyveromyces lactis* [21]. Interestingly, in the latter work, it could also be shown that species-specificity of the Mid2 sensor seems to be mainly conferred by the extracellular sequences.

In conclusion, the data presented in this work indicate that intracellular signal generation in the CWI pathway is at least partially governed by the local concentrations of the sensors Wsc1 and Mid2 within the plasma membrane. These are determined by the cytoplasmic sensor tails. For Wsc1 it could be shown that the determinant for plasma membrane localization within the cytoplasmic tail is an endocytosis signal [26]. For Mid2, the processes determining the static localization within the plasma membrane remain to be elucidated.

Acknowledgements: Hans-Peter Schmitz was of invaluable help with all aspects of fluorescence microscopy. We are also grateful to Rosaura Rodicio for critical reading of the manuscript. This work has been funded by a Grant from the Deutsche Forschungsgemeinschaft to J.J.H. (SFB 431).

References

[1] Bowman, S.M. and Free, S.J. (2006) The structure and synthesis of the fungal cell wall. Bioessays 28, 799–808.
[2] Carrillo-Munoz, A.J., Guisiano, G., Ezkurra, P.A. and Quindós, G. (2006) Antifungal agents: mode of action in yeast cells. Rev. Esp. Quimoterap. 19, 130–139.
[3] Klis, F.M., Boorsma, A. and De Groot, P.W. (2006) Cell wall construction in *Saccharomyces cerevisiae*. Yeast 23, 185–202.
[4] Heinisch, J.J. (2005) Baker's yeast as a tool for the development of antifungal kinase inhibitors – targeting protein kinase C and the cell integrity pathway. Biochim. Biophys. Acta 1754, 171–182.
[5] Levin, D.E. (2005) Cell wall integrity signaling in *Saccharomyces cerevisiae*. Microbiol. Mol. Biol. Rev. 69, 262–291.
[6] Roncero, C. and Duran, A. (1985) Effect of Calcofluor white and Congo red on fungal wall morphogenesis: In vivo activation of chitin polymerization. J. Bacteriol. 163, 1180–1185.
[7] Straede, A., Corran, A., Bundy, J. and Heinisch, J.J. (2007) The effect of tea tree oil and antifungal agents on a reporter for yeast cell integrity signalling. Yeast 24, 321–334.
[8] Gray, J.V., Ogas, J.P., Kamada, Y., Stone, M., Levin, D.E. and Herskowitz, I. (1997) A role for the Pkcl MAP kinase pathway of *Saccharomyces cerevisiae* in bud emergence and identification of a putative upstream regulator. EMBO J. 16, 4924–4937.
[9] Jacoby, J.J., Nilius, S.M. and Heinisch, J.J. (1998) A screen for upstream components of the yeast protein kinase C signal

transduction pathway identifies the product of the *SLG1* gene. Mol. Gen. Genet. 258, 148–155.
[10] Verna, J., Lodder, A., Lee, K., Vagts, A. and Ballester, R. (1997) A family of genes required for maintenance of cell wall integrity and for the stress response in *Saccharomyces cerevisiae*. Proc. Natl. Acad. Sci. USA 94, 13804–13809.
[11] Ketela, T., Green, R. and Bussey, H. (1999) *Saccharomyces cerevisiae* Mid2p is a potential cell wall stress sensor and upstream activator of the *PKC1–MPK1* cell integrity pathway. J. Bacteriol. 181, 3330–3340.
[12] Lommel, M., Bagnat, M. and Strahl, S. (2004) Aberrant processing of the WSC family and Mid2p cell surface sensors results in cell death of *Saccharomyces cerevisiae O*-mannosylation mutants. Mol. Cell. Biol. 24, 46–57.
[13] Rajavel, M., Philip, B., Buehrer, B.M., Errede, B. and Levin, D.E. (1999) Mid2 is a putative sensor for cell integrity signaling in *Saccharomyces cerevisiae*. Mol. Cell. Biol. 19, 3969–3976.
[14] Lodder, A.L., Lee, T.K. and Ballester, R. (1999) Characterization of the Wscl protein, a putative receptor in the stress response of *Saccharomyces cerevisiae*. Genetics 152, 1487–1499.
[15] Green, R., Lesage, G., Sdicu, A.M., Menard, P. and Bussey, H. (2003) A synthetic analysis of the *Saccharomyces cerevisiae* stress sensor Mid2p, and identification of a Mid2p-interacting protein, Zeolp, that modulates the *PKC1–MPK1* cell integrity pathway. Microbiology 149, 2487–2499.
[16] Philip, B. and Levin, D.E. (2001) Wscl and Mid2 are cell surface sensors for cell wall integrity signaling that act through Rom2, a guanine nucleotide exchange factor for Rhol. Mol. Cell. Biol. 21, 271–280.
[17] Arvanitidis, A. and Heinisch, J.J. (1994) Studies on the function of yeast phosphofructokinase subunits by *in vitro* mutagenesis. J. Biol. Chem. 269, 8911–8918.
[18] Wach, A., Brachat, A., Alberti Segui, Rebischung, C. and Philippsen, P. (1997) Heterologous *HIS3* marker and GFP reporter modules for PCR-targeting in *Saccharomyces cerevisiae*. Yeast 13, 1065–1075.
[19] Longtine, M.S., McKenzie 3rd, A., Demarini, D.J., Shah, N.G., Wach, A., Brachat, A., Philippsen, P. and Pringle, J.R. (1998) Additional modules for versatile and economical PCR-based gene deletion and modification in *Saccharomyces cerevisiae*. Yeast 14, 953–961.
[20] Sheff, M.A. and Thorn, K.S. (2004) Optimized cassettes for fluorescent protein tagging in *Saccharomyces cerevisiae*. Yeast 21, 661–670.
[21] Rodicio, R., Buchwald, U., Schmitz, H.P. and Heinisch, J.J. (in press) Dissecting sensor functions in cell wall integrity signaling in *Kluyveromyces lactis*, Fungal Genet. Biol., doi:10.1016/j.fgb.2007.07.009.
[22] Lorberg, A., Jacoby, J.J., Schmitz, H.P. and Heinisch, J.J. (2001) The PH domain of the yeast GEF Rom2p serves an essential function *in vivo*. Mol. Genet. Genomics 266, 505–513.
[23] Vay, H.A., Philip, B. and Levin, D.E. (2004) Mutational analysis of the cytoplasmic domain of the Wscl cell wall stress sensor. Microbiology 150, 3281–3288.
[24] Markovich, S., Yekutiel, A., Shalit, I., Shadkchan, Y. and Osherov, N. (2004) Genomic approach to identification of mutations affecting caspofungin susceptibility in *Saccharomyces cerevisiae*. Antimicrob. Agents Chemother. 48, 3871–3876.
[25] Serrano, R., Martin, H., Casamayor, A. and Arino, J. (2006) Signaling alkaline pH stress in the yeast *Saccharomyces cerevisiae* through the Wscl cell surface sensor and the Slt2 MAPK pathway. J. Biol. Chem. 281, 39785–39795.
[26] Piao, H.L., Machado, I.M. and Payne, G.S. (2007) NPFXD-mediated endocytosis is required for polarity and function of a yeast cell wall stress sensor. Mol. Biol. Cell 18, 57–65.